GEODETIC DEFORMATION OF FUEGO VOLCANO THROUGH GEOSPATIAL DATA FROM 2015 TO 2025

MOLINA MONTERO NOELIA DE LOS ANGELES[1]

Supervisors: Yohei KINOSHITA[2]**, Saeko KITA**[3]

ABSTRACT

This investigation focuses on the eruptive dynamics and surface deformation of Fuego Volcano in Guatemala between 2015 and 2025, a period marked by an increase in volcanic activity and the availability of satellite data. The main objective is to monitor the geodetic deformation of Fuego Volcano using geospatial data collected from 2015 to 2025. The methodology utilizes Sentinel-1 satellite data, which include ascending and descending orbital paths, along with InSAR, to identify deformation. Statistical analysis techniques such as linear regression and Savitzky-Golay filtering were employed. The displacement time series was analyzed using the LiCSBAS, which utilizes the NSBAS algorithm.

The results enabled an analysis of the cyclical eruptive behavior of Fuego Volcano, identifying periods of calm and active moments. Significant inflation was observed at Fuego Volcano. This study enhances our understanding of volcanic dynamics and illustrates the importance of satellite-based techniques for improving hazard assessment. In the future, we expect to conduct monitoring of volcanoes in Central America using a combination of the InSAR Data, paroxysmal events, and seismic activity.

Keywords: Fuego Volcano, Pacaya Volcano, Paroxysmal, LiCSBAS, Sentinel -1.

1. INTRODUCTION

Fuego Volcano is situated at the convergence of three major tectonic plates, the Cocos, Caribbean, and North American plates; this complex geodynamic condition and its high elevation contribute to the region's unique geological characteristics and the exposition of natural phenomena such as seismicity and volcanic activities (Burkart & Self, 1985); with this last case, Guatemala is part of the Central American Volcanic Arc System (CAVAS), which has some of the most dangerous volcanoes of Central America (Pedol, 2019). Between 2015 and 2025, Fuego Volcano exhibited frequent eruptive activity, including effusive and explosive phases. One of the most catastrophic events occurred on June 3, 2018, resulting in significant loss of life and widespread destruction. Fuego Volcano entered a new eruptive phase in 2015, with increased paroxysmal eruptions. These eruptions are events, including the continuous effusion of lava flows, explosive activity, and an intense eruptive phase. This culminated in a sustained eruptive column, accompanied by pyroclastic flows and a gradual decline in explosive activity (Naismith et al., 2019). Additionally, Pacaya Volcano is a composite complex volcano predominantly composed of basalt, dacite, rhyolite, and basaltic andesite (INSIVUMEH, 2024). It is located within a subduction zone, with its last eruption in August 2021. Historically, Pacaya has experienced Strombolian eruptions, which are marked by a continuous flow of lava that has partially covered the flanks of the Mackenney cone. Additionally, the volcano has undergone significant explosive eruptions that have destroyed its summit (Global Volcanism Program, 2024). In the present study, in order to monitor the deformation of Pacaya and Fuego volcanoes, we applied Synthetic Aperture Radar (SAR) Interferometry (InSAR). SAR data can be acquired during ascending (satellite moves from south to north) or descending (from north to south) orbital paths, each providing a distinct

[1] Volcanes sin Fronteras (VSF), Costa Rica.
[2] Satellite Geodesy Research Laboratory, University of Tsukuba.
[3] International Institute of Seismology and Earthquake Engineering, Building Research Institute.

line-of-sight geometry. In this context, geospatial technologies, such as remote sensing, have significantly advanced risk and disaster management monitoring strategies, with SAR techniques being particularly effective.

2. DATA

For this study, we used several parameters to analyze geospatial information, including Digital Elevation Model (DEM), Sentinel-1, and Looking Into Continents from Space (LiCSAR) with SAR. In the specific case of Fuego Volcano, we also used the historical volcanic eruption data, focusing primarily on explosive events classified as paroxysmal eruptions, as well as historical seismic eruptions.
The development of LiCSAR is valuable because it efficiently extracts data from preprocessed interferograms. The COMET-LiCS Sentinel-1 InSAR platform provides access to LiCSAR results and manages the large daily data output from the Sentinel-1 satellite constellation (Morishita et al., 2016).

3. METHODOLOGY

3.1. Process in LiCSBAS

To investigate the displacement deformation at the Fuego and Pacaya volcanoes, we employed LiCSBAS (Morishita et al., 2020) in conjunction with LiCSAR products spanning the period from 2015 to 2025. We acquired an interferometric dataset that comprised unwrapped phase data, line of sight geometry (LOS), and GeoTIFF products for both ascending and descending tracks from the COMET-LiCS portal. The data were converted to binary format and processed through multilooking to enhance spatial coherence and minimize noise.

The time series analysis was conducted using the Short Baseline Subset (SBAS) inversion method, incorporating the Non-Short Baseline Subset (NSBAS) approach to address temporal gaps. Bootstrap resampling was utilized to estimate values and eliminate pixels with low reliability. Subsequently, a spatiotemporal filtering step was implemented to reduce atmospheric artifacts and enhance the detection of long-term deformation signals.

3.2. Statistical post-processing for obtained deformation

Data visualization and analysis were performed using Jupyter Notebook, leveraging the h5py library for efficient management of large HDF5 datasets. The LiCSBAS command TS_GEOCml1maskclip was executed for each study area and acquisition geometry to produce masked time series products. These outputs were then analyzed using cumulative displacement files (cum.h5), allowing for both temporal and spatial exploration of deformation patterns through maps and line-of-sight displacement graphs. At this stage, no additional masking was applied to retain peripheral deformation features that could be significant to volcanic activity.

Linear regression was employed to estimate deformation rates, following the model:

$$y = mx + b \qquad (1)$$

Where “y” is the dependent variable (vertical displacement), “x” is the independent variable (time), “m” represents the slope representing the average deformation, and “b” indicates where the line crosses the “y” axis (Dagnino, 2014).

The Savitzky-Golay filter effectively reduces high-frequency noise, facilitates smoothing, and assists in differentiation. This method was applied solely for visualization purposes and did not alter the data (Gallagher, 2020).

As part of this investigation, the use of LiCSBAS and LiCSAR methodologies was analyzed and validated in the context of Pacaya Volcano. This analysis aims to enhance our understanding of

volcanic activity and improve the accuracy of remote sensing techniques for the assessment of geophysical phenomena.

4. RESULTS AND DISCUSSION

In this section, we will present the findings from our analysis of volcanic deformation, utilizing Sentinel-1 data processed through LiCSBAS to Fuego and Pacaya Volcanoes. We also focus on the paroxysmal events of Fuego Volcano. This chapter aims to critically evaluate these results and discuss the advantages of using open-source resources in our research.

Figure 1. The total context of the study

4.1. Fuego Volcano: paroxysmal events

On June 3, 2018, the Fuego volcano erupted, affecting around 12,000 people and resulting in 113 fatalities and 332 missing individuals. The area of El Rodeo was particularly impacted (Bartel, 2023). Ash reached altitudes of 9 kilometers, while pyroclastic currents traveled up to 10 kilometers down the slope, driven by ongoing eruptions and a partial collapse of the volcano's structure (De Angelis et al., 2018).

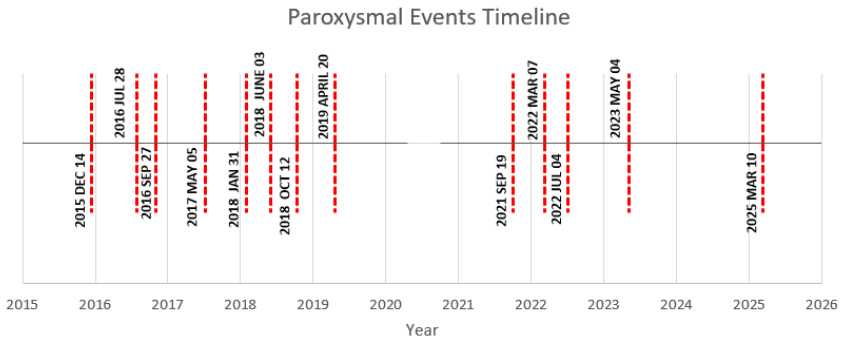

Figure 2. Graphic of the most significant Paroxysmal events. The most significant paroxysmal events during 2015 to 2025, were based on the Global Volcanism Program (2025).

Fuego Volcano has experienced multiple paroxysms of varying scales, and since 2015, it has entered a new eruptive period marked by consistent daily activity (Pardini et al., 2019; Naismith et al., 2019). We will analyze paroxysms classified as "major," which are notably violent eruption events of the volcano (Zobin, 2018).

Figure 2 shows the behavior of paroxysmal events from 2015 to 2025. Before June 3, 2018, there were nearly three years without major events. A notable eruption occurred six months before the severe 2018 event, with another significant incident about four months later. The last event was on April 20, 2019, followed by a 1.5-year calm period. From 2021 to 2023, paroxysmal events increased again, with nearly two years of calm before new activity began in 2025.

Naismith et al. (2019) analyze the eruptive frequency patterns of Fuego Volcano, noted for its activity since 1999. The authors highlight that the highest explosive activity occurs at the summit, alongside effusive lava flows and a series of explosive events. During intense eruptive phases, continuous explosions and pyroclastic flows happen in 24 to 48-hour cycles, producing significant eruptive columns. Following this activity, the explosive behavior decreases.

In summary, there are cyclic dynamic eruptivities in Fuego Volcano, which commonly alternate between very active periods and intervals of calm stages.

4.2. Fuego Volcano Ascending and Descending outcome

Figure 3(a) displays velocity ranges in millimeters per year, from -30 mm/year (blue) to 10 mm/year (red). The average data collected over 10 years indicates that the warm colors (red) suggest ground uplift in the regions around the crater and its flanks.

The results in Figure 3(b) show that the average displacement velocity shows a uniform color distribution around the crater and its flanks. However, in the western area of Fuego Volcano, some pixels have negative values, likely due to data noise or volcanic ash fallout.

We selected Acatenango Volcano as our reference point because it is stable and classified as inactive, with its last eruption in 1972. This location exhibits high coherence, like Pacaya Volcano, supporting our choice due to Acatenango's inactive status (Bedón et al., 2024).

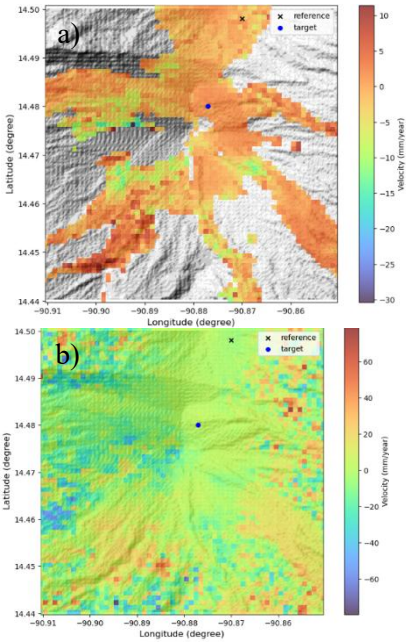

Figure 3. Fuego Volcano illustrates the orbital ascending (a), and descending (b) interferometric displacement observed from 2015 to 2025.

4.3. Fuego Volcano Ascending and Descending graphics outcome

The results from the cumulative relative displacement analysis indicate that Fuego Volcano experienced an average uplift velocity of 1.43 mm/year. However, the data is somewhat noisy, and this variability may be related to a shift in the volcano's eruptive regime that began in 2015, marking the start of a new and more active eruptive phase (Naismith et al., 2019) during the study period (see Figure 4).

In contrast, the cumulative relative displacement observed from 2015 to 2017 shows an average velocity of 7.24 mm/year, although the results appear relatively weak, with only a few blue dots present. Nevertheless, this data has remained consistent over the years. As illustrated in Figure 5, we can see the details of the cumulative relative displacement, which confirms an average velocity of 7.24 mm/year. While the interferometry data from 2015 to 2017 exhibited weak results with limited visible blue dots, it has maintained consistency over time.

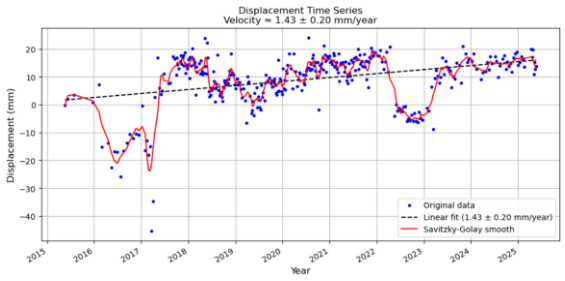

Figure 4. Cumulative relative displacement ascending with average linear velocity and confidence in Fuego Volcano.

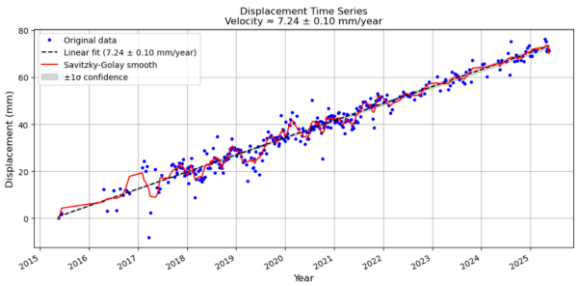

Figure 5. Cumulative relative displacement descending with average linear velocity and confidence in Fuego Volcano.

4.4. Pacaya Volcano Ascending and Descending outcome

Figure 6(a) shows the velocity displacement from 2015 to 2025, with a maximum annual uplift of 4 mm and a minimum of -12 mm. In Pacaya Volcano, a shift from blue to red indicates that it is moving away from the satellite, demonstrating subsidence and eastward displacement.

Figure 6(b) reveals a maximum uplift of approximately 0 mm/year and a minimum of about -25 mm/year. The color changes suggest variations in distance from the satellite. Reference and target points were established for analyzing displacement; the reference point is in a stable crop area, while the target point is in a deformed region. Figures 7 and 8 visually represent the data and suggest specific behaviors in the study area.

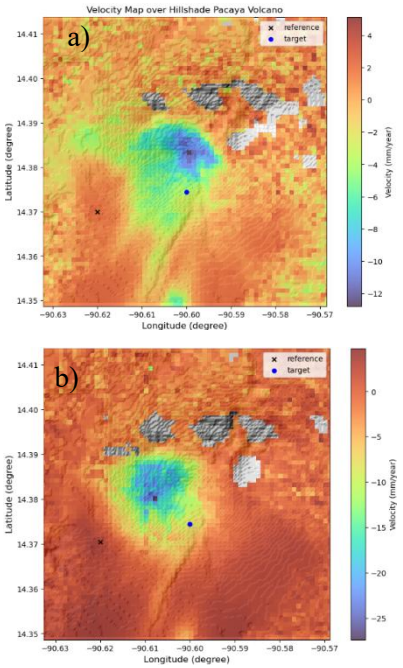

Figure 6. Fuego Volcano illustrates the orbital ascending (a), and descending (b) interferometric displacement observed from 2015 to 2025.

4.5. Pacaya Volcano Ascending and Descending graphics outcome

The graphical data shows displacement in millimeters from 2015 to 2025. The cumulative displacement over this ten-year period is approximately 62.9 mm, resulting in an average annual velocity of -6.29 mm (see Figure 7). In the descending orbit, the cumulative relative displacement is around 110.5 mm, with a subsidence rate of -11.05 mm per year (Figure 8). The gap in the data from 2022 to 2023 is likely due to the absence of satellite acquisition.

The results indicate a trend of deflation at Pacaya Volcano from 2015 to 2025, which was observed in the ascending and descending time-series data. The analyzed information reveals significant subsidence, which is likely associated with a reduction in volume and structural instability within the volcanic edifice. These findings are consistent with prior research that identified long-term instability in the southwestern flank, even before 2015 (Gonzalez-Santana & Wauthier, 2021).

Another document provides a detailed account of the period from 2007 to 2020, highlighting the explosive flank slide eruption that occurred in 2010. During this event, the slide opened and accelerated, ultimately moving toward the southwest area, which is also the focus of this study. The deformation pattern in this region appears to be persistent and may be influenced by an active décollement fault, allowing for continued movement of the flank (Gonzalez-Santana et al., 2022).

However, remote sensing will have certain limitations from 2022 to 2023. Consequently, it is essential to augment satellite-based observations with ground-based monitoring systems to enhance risk assessments and identify potential reactivation that could lead to future eruptive activity (Gonzalez-Santana et al., 2024).

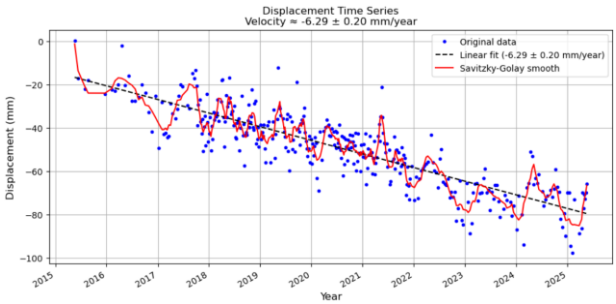

Figure 7. Cumulative relative displacement ascending with average linear velocity and confidence in Pacaya Volcano.

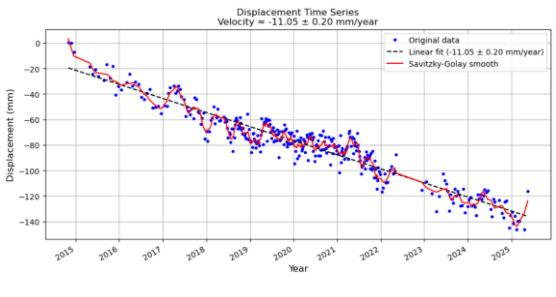

Figure 8. Cumulative relative displacement descending with average linear velocity and confidence in Pacaya Volcano.

5. CONCLUSIONS

The present study examined geodetic deformation related to both active and calm periods at Fuego Volcano, based on results of InSAR analysis by LiCSBAS in the period of 2015 to 2025. We identified a cyclical eruptive dynamic at Fuego Volcano. It is commonly a period of very high activity with some calm periods.

During a 10-year monitoring period of Fuego Volcano, observations from a descending orbit indicated an inflation rate of 7.24 mm per year. Despite this, the data also revealed an average uplift velocity of 1.43 mm per year over the study period. Despite the limitations of Sentinel-1 data, it was possible to obtain valuable data, particularly for understanding the dynamics of Fuego Volcano and establishing a relationship with seismic and eruptive phenomena.

The Pacaya Volcano was used to validate our data. We found consistent deflation information that matched scientific articles from the study period. This is significant since both Pacaya and Fuego Volcanoes are in the same Sentinel-1 Frame ID.

From 2015 to 2025, the Pacaya Volcano had a total displacement of about 100 mm during the ascending phase, with an average annual movement of -6.29 mm. In the descending phase, it experienced a cumulative displacement of around 140 mm, with an average subsidence of -11.05 mm per year.

ACKNOWLEDGEMENTS

This research was conducted during the individual study period of the training course "Seismology, Earthquake Engineering, and Tsunami Disaster Mitigation," organized by the Building Research Institute, JICA, and GRIPS. I wish to extend my heartfelt gratitude to my supervisor, Dr. Yohei Kinoshita, for his invaluable support. Additionally, I would like to recognize Dr. Saeko Kita and Dr. Tatsuhiko Hara for their support throughout the entire program.

REFERENCES

Bartel, B. A. (2023). *Guatemala* Michigan Technological University].

Bedón, P. A. E., Ebmeier, S. K., Elliott, J. R., Wright, T. J., Mothes, P., Cayol, V.,…Andrade, D. (2024). Journal of Volcanology and Geothermal Research, 454, 108147.

Burkart, B., & Self, S. (1985). *Geology*, *13*(1), 22-26.

Dagnino, J. (2014). *Revista Chilena de Anestesia*, *43*(2), 143-149.

De Angelis, S., Chigna, G., Ripepe, M., Gonzalez, D., Lockhart, A. B., Juarez, F.,…Munkli, B.-H. (2018).

Gallagher, N. B. (2020). *Eigenvector Research Incorporated*, *2*, 4.

Global Volcanism Program (2024). . Distributed by Smithsonian Institution, compiled by Venzke E.

Gonzalez-Santana, J., & Wauthier, C. (2021). Journal of Volcanology and Geothermal Research, 410, 107147.

Gonzalez-Santana, J., Wauthier, C., & Burns, M. (2022). *Bulletin of Volcanology*, *84*(9), 84

Gonzalez-Santana, J., Wauthier, C., & Waite, G. (2024). Journal of Volcanology and Geothermal Research, 447, 108027.

Instituto Nacional de Sismología, Vulcanología, Meteorología e Hidrología (INSIVUMEH). (2024). Volcán de Pacaya [Folleto].

Mora, O., Ordoqui, P., Iglesias, R., & Blanco, P. (2016). Procedia Computer Science, 100, 1135-1140

Morishita, Y., Lazecky, M., Wright, T. J., Weiss, J. R., Elliott, J. R., & Hooper, A. (2020). *Remote Sensing*, *12*(3), 424.

Naismith, A. K., Watson, I. M., Escobar-Wolf, R., Chigna, G., Thomas, H., Coppola, D., & Chun, C. (2019). Journal of Volcanology and Geothermal Research, 371, 206-219.

Pedol, L. C. (2019). Revista Geofísica(69), 97-115.

Zobin, V. M. (2018). (1960–2010). *Frontiers in Earth Science*, *6*, 46.